Exosome-derived lncRNA-Ankrd26 promotes dental pulp restoration by regulating miR-150-TLR4 signaling

LIN LI and JIANPING GE

Department of Endodontics, School and Hospital of Stomatology, Tongji University, Shanghai Engineering Research Center of Tooth Restoration and Regeneration, Shanghai 200072, P.R. China

Received December 7, 2020; Accepted December 30, 2021

DOI: 10.3892/mmr.2022.12668

Abstract. At present, retaining the biological function of dental pulp is an urgent requirement in the treatment of pulp disease; it has been recognized that application of dental pulp stem cells (DPSCs) in regenerating dental pulp and dentin complexes is expected to become a safe and effective treatment of pulp disease; meanwhile the role of DPSC-derived exosomes in dental pulp regeneration and repair is gaining attention. However, the underlying mechanism of DPSCs in dental pulp regeneration and repair is still unclear. In the present study, a variety of *in vitro* biological experiments and an animal model, as well as next-generation sequencing and bioinformatics analysis, demonstrated that DPSCs promoted migration and osteoblastic differentiation of mesenchymal stem cells (MSCs) via exosomes; this was induced by DPSC-derived exosomal long non-coding (lnc)RNA-ankyrin repeat domain (Ankrd)26. Mechanistically, the effect of exosomal lncRNA-Ankrd26 on migration and osteoblastic differentiation of MSCs was dependent on microRNA (miR)-150/Toll-like receptor (TLR)4 signaling; this was regulated by lncRNA-Ankrd26. The present study demonstrated that exosomes-derived lncRNA-Ankrd26 from DPSCs promoted dental pulp restoration via regulating miR-150-TLR4 signaling in MSCs; these findings help to understand the mechanism of dental pulp repair, identify therapeutic targets in the development of pulpitis and develop clinical treatments.

Introduction

At present, root canal therapy and pulpotomy are important treatments for dental pulp injury (1); however, concomitant complications and considerable failure rate limit the widespread use of these treatments in clinical practice (2). Although current root canal filling materials, such as gutta percha and caprolactone-based points (2), have good biocompatibility and effectively seal the apical foramen, treatment often leads to destruction of dental hard tissue and loss of pulp vitality. Therefore, retaining biological function of dental pulp is an urgent requirement in the treatment of pulp disease. Dental pulp stem cells (DPSCs) have been used as seed cells in reconstruction of the dental pulp system because of their potential for multi-directional differentiation, self-renewal and angiogenesis (3). DPSCs were first isolated from the pulp of human third permanent molars and subcutaneously implanted on the back of nude mice to form a pulp-dentin-like structure in 2000 (4); studies have confirmed the ability of DPSCs to form hard tissue and dental cementum (5,6) and to induce osteogenesis in dental engineering, such as promoting osteoblast differentiation (7,8). The aforementioned studies indicate that use of DPSCs in regenerating the pulp-dentin complex and repairing damaged pulp may become a safe and effective treatment of pulp disease.

Inflammation-mediated tissue repair and regeneration are key for restoration of damaged dental pulp (9). During the repair and regeneration process, DPSCs in the microenvironment are recruited, proliferate and differentiate to repair and regenerate damaged dental pulp (10). However, the role and mechanism of DPSCs in pulp restoration is unknown and investigation is required to understand the involvement of DPSCs in pulp restoration tissue engineering. Recent studies have demonstrated that DPSC-derived exosomes are associated with inflammation-mediated pulp regeneration (11,12). Exosomes are membranous vesicles, 30-150 nm in diameter. The molecular content of exosomes is not only a fingerprint of the cell phenotype, but can be transferred to other cells and affect their biological behaviors, including intercellular communication (13). Specific molecular markers, among which the most abundant are tetraspanins including CD81, CD63 and CD9, are detected on the surface of exosomes (14). Exosomes contain proteins, genetic material and lipids; genetic components including DNA and RNAs [microRNA (miRNA or miR), long non-coding (lnc)RNA and circular RNA) are gaining attention (13,14). It has been demonstrated that dysregulated lncRNAs serve a key role in determining the function of stem cells, including stem cell pluripotency and differentiation (14);

Correspondence to: Professor Jianping Ge, Department of Endodontics, School and Hospital of Stomatology, Tongji University, Shanghai Engineering Research Center of Tooth Restoration and Regeneration, 399 Yanchang Road, Shanghai 200072, P.R. China
E-mail: gejianping@tongji.edu.cn

Key words: injury-repair, dental pulp stem cells, mesenchymal stem cells, exosomes, long non-coding RNA-Ankyrin repeat domain 26, microRNA-150, Toll-like receptor 4 signaling

moreover, lncRNAs also serve as 'sponges' to titrate miRNAs during the differentiation of stem cells (15).

By contrast, the association between lncRNAs and miRNAs in DPSCs in dental tissue repair is unclear. To comprehensively address the aforementioned issue, in the present study, a variety of *in vitro* biological experiments based on an animal model were performed, as well as next-generation sequencing and bioinformatics analysis, in order to help to broaden the application prospects of DPSCs, not only in dental tissue restoration, but also in the field of bone injury repair.

Materials and methods

Animal model. A model of pulpitis was constructed in six-week-old male Sprague-Dawley rats (weight, 180-200 g), purchased from Shanghai Laboratory Animal Company. All animals were housed in the specific-pathogen-free facility in the Institute of Hospital of Stomatology, Tongji University (Shanghai, China) and were maintained under a 12/12-h light/dark cycle with free access to rodent chow and water at room temperature under a controlled humidity (50±10%). A total of 12 rats were randomly divided into two groups: Control group and pulp injury model group, with 6 rats in each group. These animals were placed in a sealed container with a 4% (vol/vol) isoflurane flow until fully anaesthetized, then their mandibular incisor labial pulp tissues were resected by an electrosurgical generator, following which the surgical wounds were dressed. The diameter of gingival defects was >5 mm, deep to hard tissue. All pulp tissue was extracted on the 30th day after modeling and prepared for histomorphometry and statistical analysis. All animals were sacrificed with CO_2 asphyxiation in a chamber (100% CO_2, 9.6 l/min, 10 min) followed by cervical dislocation to confirm death. All animal experiments were approved by the Institutional Animal Care and Use Committees of the Hospital of Stomatology, Tongji University (approval no. 20180606; Jan 1, 2018); studies were performed in adherence with the international Guide for the Care and Use of Laboratory Animals.

Primary culture and identification of DPSCs. Pulp tissue was removed under aseptic conditions, washed with 0.01 M sterile PBS and cut into small pieces (~1.0 mm^3). Following digestion at 37˚C for 1 h with 0.3% type I collagenase and 0.4% dispase, discrete single cell clumps were pipetted, then the formed single cell suspension was filtered through a cell sieve (70-μm pore size) and centrifuged at 300 x g for 5 min at room temperature. After washing the cells with 1X PBS, the cell precipitate was resuspended in high glucose DMEM containing 20% FBS (Gibco; Thermo Fisher Scientific, Inc.), and inoculated into a 5 ml culture flask at a density of $5x10^4$ cells/ml for routine culture at 37˚C in a humidified atmosphere of 5% CO_2/95% air. The medium was changed every 3 days, and cells in the logarithmic growth phase were collected. The culture supernatant was centrifuged at 2,000 x g for 10 min at 4˚C, filtered (filter diameter, 0.22 μm) and mixed with high glucose DMEM containing 10% FBS (Gibco; Thermo Fisher Scientific, Inc.) at a ratio of 1:1 for clonal culture medium. The first-generation cells in the logarithmic growth phase were diluted with adaptive medium to 10-15 cells/ml; cells were inoculated in a 96-well plate (100 μl/well) for 12 h at 37˚C in a humidified atmosphere of 5% CO_2/95% air and medium was changed every 5 days. When the cells start to grow, the medium was changed every 3 days. Identification of DPSCs was performed by morphological detection using an inverted phase contrast microscope (CKX53FL; Olympus) and specific marker labeling, including CD34, CD45, CD29 and CD44, as described previously (16).

Isolation and identification of DPSC-derived exosomes. To remove cellular debris, medium from DPSCs was centrifuged at 2,500 x g for 15 min at 4˚C and filtered with a 0.22 μm filter. The collected medium containing exosomes was laid on top of a 30% sucrose/D_2O cushion in a sterile UltraClear™ (Beckman Coulter, Inc.) and ultracentrifuged at 100,000 x g for 1 h at 4˚C. The pellets were resuspended in 15 ml PBS and centrifuged at 4,000 x g at 4˚C for 15 min until the volume was concentrated to ~200 μl. The total number of exosomes was determined using CD63 ExoELISA™ (System Biosciences Inc.) according to the manufacturer's instructions. Exosomes were identified by dynamic light scattering analysis and transmission electron microscopy (TEM) according to a previous study (17). Briefly, an enriched exosome suspension in filtered PBS solution was dispensed on carbon-coated electron microscopy grids on parafilm and left to absorb for 10 min at room temperature, then transferred to a drop of Uranyless® solution (Electron Microscopy Sciences) for 1 min and left to air dry. Excess stain was blotted away. Imaging was performed with a Jeol JEM-2200FS microscope (Jeol, Ltd.) at 200 kV. Moreover, the expression of CD63 and CD81 or GM130 and calnexin was evaluated by western blotting. RNA and proteins were extracted for further analysis using a Total Exosome RNA & Protein Isolation kit (Thermo Fisher Scientific, Inc.). To determine the effect of DPSCs on the migration and osteoblastic differentiation of mesenchymal stem cell (MSCs), rat MSCs were obtained from Nanjing Cell Life Biotechnology Co., Ltd. The isolation and purification of rat MSCs was performed as previously described (16). MSC medium (cat. no. #7501) was obtained from ScienCell Research Laboratories, Inc. and cultured MSCs in conditioned medium from DPSCs.

Microarray-based differential profiling and bioinformatics analysis. Total RNA was isolated from the pulp samples of rats using TRIzol® (Invitrogen; Thermo Fisher Scientific, Inc.) according to the manufacturer's protocol. The microarray hybridization was performed using total RNA prepared as aforementioned. Gene set enrichment analysis (GSEA) tested whether an *a priori* defined set of genes shows statistically significant, concordant differences. The uploaded gene set consisted of normalized mRNA expression data and was sorted by the mean log2 signal ratios. Small RNAs of DPSC-derived exosomes were extracted and used for miRNA sequencing with Illumina HiSeq 2500 platform at Yunxu Co. Ltd. The aggregated distribution of gene expression levels in pathways was determined by normalized enrichment score, which represented statistical significance following enrichment analysis. The KEGG database (http://www.genome.jp/kegg/) was used for pathway annotation. Pathways that were significantly biased in the control and model group were identified.

lncRNA-Ankyrin repeat domain (Ankrd)26 and miRNA-150 mimic and inhibitor transfection. Cells were cultured in DMEM supplemented with 10% FBS (both Gibco; Thermo Fisher Scientific, Inc.). The cells were cultured at 37˚C in a humidified atmosphere of 5% CO_2. Transfection with lncRNA-Ankrd26 and miRNA-150 mimic and inhibitor were with 30 nM concentration at room temperature performed using Lipofectamine® 3000 (Invitrogen; Thermo Fisher Scientific, Inc.) according to the manufacturer's protocols. After 48 h of transfection, the cells were harvested for reverse transcription-quantitative (RT-q)PCR analysis and western blotting. All transfections were confirmed with appropriate controls, including mimic negative control or inhibitor negative control. The transfection efficacy was confirmed (Figs. S1 and S2). The sequence information is listed in Table SI.

TLR4 knockdown. The short hairpin RNA (shRNA) carrier was constructed to target the *tlr4* gene by respectively inserting three different target sequences into the plasmid pLKO.1 (catalog no. 10878; Addgene, Inc.). In brief, lentiviral vectors pLKO.1 TRC and pWPI.1 were used for constructing recombinant lentiviruses of short interference RNA (shRNA) constructs and TLR4 shRNA, non-targeting shRNA (shNT). Recombinant lentivirus was amplified in 293T cells. After transfection, MSCs cells with TLR4 knockdown were screened and obtained for subsequent detection with western blotting or migration assay.

Migration assay. The migratory capacity of DPSCs with/without exosomal inhibitor (GW4869) (catalog no. HY-19363; MedChemExpress) or shTLR4 treatment was tested using a Transwell Boyden Chamber (6.5-mm; Costar) with polycarbonate membranes (8-μm pore size) on the bottom of the upper compartment. Cells were seeded in the upper chamber at a density of $5x10^4$ cells/well with serum-free high-glucose DMEM; the lower chamber was filled with 600 μl high-glucose DMEM containing 20% FBS (Gibco; Thermo Fisher Scientific, Inc.). At the end of the incubation at 37˚C for 48 h, the cells that penetrated through to the lower surface of filter membranes were fixed with 90% ethanol for 15 min at room temperature and stained with 0.1% crystal violet solution for 5 min at room temperature. The stained cells were counted under a light microscope at x100 magnification (Olympus Corporation).

Dual-luciferase reporter assay. TargetScan online database (http://www.targetscan. org/vert_71/) was used to predict target genes for miR-150. The sequences of the TLR4 wild-type (WT) and mutant (Mut) *tlr4* gene were cloned and inserted into the 3' untranslated region (UTR) of the pEZX-MT01 vector (GeneCopoeia, Inc.). In six-well plates, 293T cells were cultured to ~70% confluence and co-transfected with WT or Mut luciferase reporter vector (2 μg) and mimic miRNAs or negative control (NC; 2 μg) using Lipofectamine 3000 (Invitrogen; Thermo Fisher Scientific, Inc.) according to the manufacturer's protocols. After 48 h, luciferase activity was detected using a Dual-Luciferase® Reporter Assay System (Promega Corporation) and normalized to *Renilla* activity. The sequence information is listed in Table SI.

Ribonucleoprotein immunoprecipitation (RIP) assay. The RIP assay was performed using the Magna RIP™ Quad RNA-Binding Protein Immunoprecipitation Kit (Merck KGaA). The cells transfected with miR-150 mimic or control were lysed using RIP lysis buffer and then 100 μl of the lysate was incubated with RIP immunoprecipitation buffer containing magnetic beads, conjugated with anti-Argonaute-2 (Ago2) G beads (catalog no. 07-590) at 4˚C for 90 min. Beads conjugated to human anti-Ago2 antibody or control IgG antibody were centrifugated at 600 x g for 1 min and then washed with RIPA buffer; after being resuspended in 50 mM Tris-HCl (pH 7.0), the beads were finally incubated at 70˚C for 45 min. RNA was extracted using TRIzol (Invitrogen; Thermo Fisher Sientific, Inc.) following the manufacturer's instructions and then quantified by RT-qPCR.

RT-qPCR. Total RNA was extracted from the cultured cells and tissue using TRIzol (Invitrogen; Thermo Fisher Scientific, Inc.) according to the manufacturer's protocols. The expression of miRNA was tested using Mir-X miRNA First Strand Synthesis and Mir-X miRNA qRT-PCR SYBR kit (Takara Biotechnology Co., Ltd.). The expression of TLR4 was tested using Transcriptor First Strand cDNA Synthesis kit and FastStart Universal SYBR Green Master (Roche Diagnostics). The amplification protocol was performed as follows: 1 cycle of 15 min at 95˚C and a further 40 cycles of 15 sec at 95˚C and 1 min at 60˚C. GAPDH was used as the housekeeping gene for normalization of the cDNA quantities. All reactions were performed in triplicate. Data were analyzed according to the $2^{-\Delta\Delta Cq}$ method (18). The sequence information is listed in Table SI.

Western blotting. Protein from cells, including DPSCs or MSCs, with a variety of treatments, and pulp tissue from rats, was extracted using RIPA buffer containing protease and phosphatase inhibitors (Beyotime Institute of Biotechnology). The protein content of the lysate was determined using the BCA protein assay (Beyotime Institute of Biotechnology). A total of 20 μg protein/lane was separated by 10% SDS-PAGE; then transferred onto PVDF membranes. Following blocking with 5% BSA for 1 h at room temperature, membranes were incubated with primary antibodies (TLR4, 1:1,000; OCN, 1:1,000; OPN, 1:1,000; RUNX2, 1:1,000; CD36, 1:1,000; CD81, 1:1,000; GM130, 1:1,000; Galnexin, 1:1,000; β-actin, 1:5,000; GAPDH, 1:1,000) at 4˚C overnight followed by incubation with horseradish peroxidase-conjugated secondary antibodies for 1 h. Blots were visualized using SuperSignal West Pico Chemiluminescent Substrate (Thermo Fisher Scientific Inc.). Results were normalized to β-actin or GAPDH. All experiments were performed three times. Quantification of western blots was analyzed densitometrically using QuantityOne software (Bio-Rad Laboratories, Inc.). The antibody information is listed in Table SII.

Statistical analysis. Statistical analysis was performed using GraphPad 11.0 (GraphPad Software, Inc.). For comparison of quantitative variables between groups, one-way ANOVA followed by Bonferroni's post hoc test for multiple comparisons or Mann-Whitney test was used. For difference in proportions between groups, χ^2 test was performed. The association

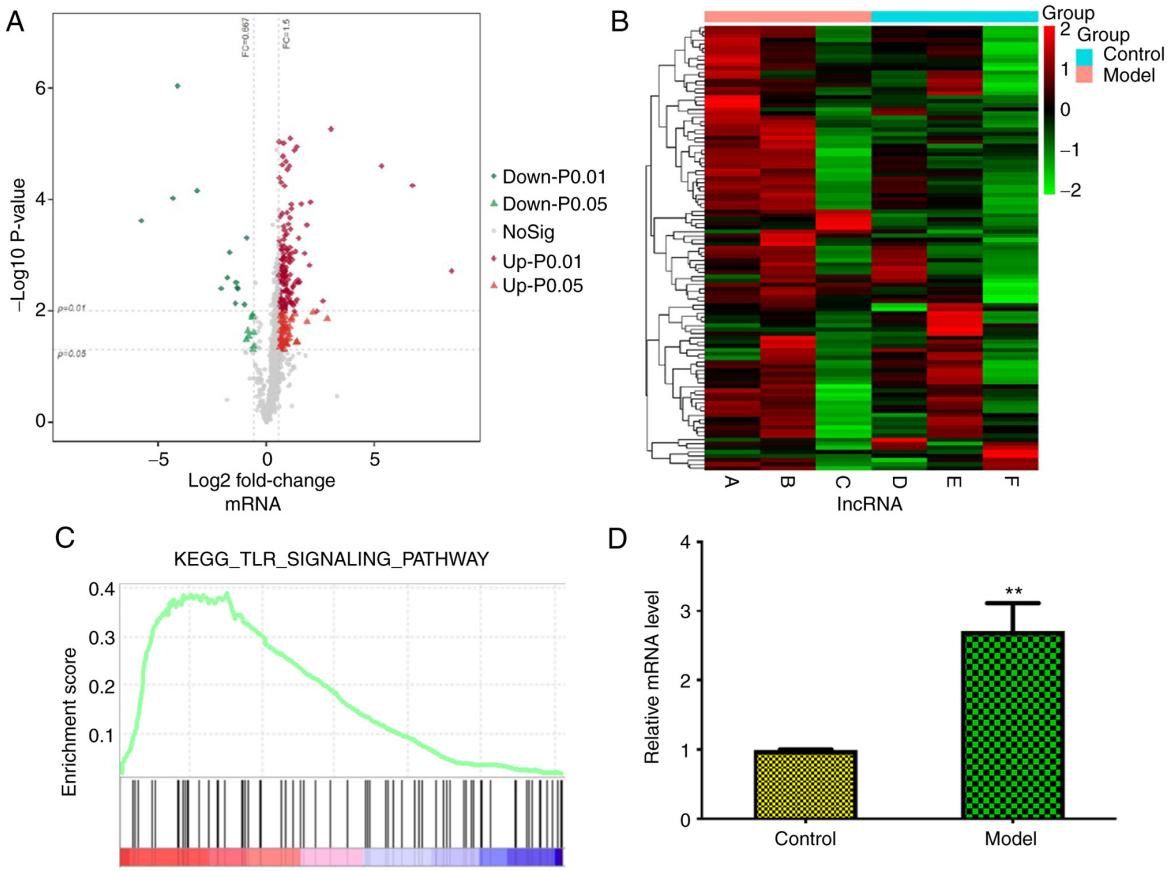

Figure 1. Dysregulated mRNAs, lncRNAs and activated TLR signalling pathway during repair and regeneration of damaged dental pulp. (A) Dysregulated mRNAs. The top ten upregulated and downregulated mRNAs are displayed in heatmap. (B) Dysregulated lncRNAs. (C) Distribution of significantly biased KEGG pathways; TLR signalling pathway was upregulated. (D) TLR4 was most significantly upregulated in the model group, which was confirmed by quantitative PCR. **P<0.01 compared with control group. The results are presented as the mean ± standard deviation. lnc, long non-coding; TLR, Toll-like receptor; KEGG, Kyoto Encyclopedia of Genes and Genomes.

between the various factors was determined using Pearson's correlation. The independent assay was performed repeatedly three times. Data are presented as the mean ± SD. P<0.05 was considered to indicate a statistically significant difference.

Results

Association between mRNAs, lncRNAs and TLR signaling pathway during repair and regeneration of pulp following injury. The present study compared next-generation sequencing mRNA and lncRNA profiles of control and pulp injury tissue from a gingival repair rat model and identified 10 significantly up- and downregulated mRNAs and lncRNAs ranked by fold-change value (Fig. 1A and B), such as AABR07015654, lnc102549726, AABR07026473 and lncRNA-Ankrd26, among which lncRNA-Ankrd26 represented notably with gradual increasing expression during the generation of a rat model. GSEA analysis showed that these significantly altered mRNAs were enriched in 'Toll-like receptor signaling pathway' (Fig. 1C); among these mRNAs, TLR4 was most highly expressed, which was confirmed by qPCR (Fig. 1D). In addition, analysis of the enrichment map showed 'TLR signaling pathway' contained genes which overlapped with six other pathways. The gene co-expression network displayed an association between lncRNA-Ankrd26 and TLR4 (Fig. 2A and B). Moreover, correlation analysis showed lncRNA-Ankrd26 was positively linearly associated with mRNA levels of TLR4 (Fig. 2C). To identify the association between lncRNA-Ankrd26 and TLR4, potential miRNAs targeting Ankrd26 and TLR4 were investigated. miR-150 was identified to be involved in the association between Ankrd26 and TLR4 (Fig. 2D). Expression of miR-150 was negatively associated with expression of both lncRNA-Ankrd26 and TLR4 in model pulp tissue (Fig. 2E and F). The results suggested that the lncRNA-Ankrd26-miR-150-TLR4 axis could play a crucial role in the repair and regeneration of injury pulp tissues.

DPSCs promote migration and osteoblastic differentiation of MSCs via exosomes. The seeded DPSCs began to grow in 24 h. The primary cells were relatively single, short spindle-like or round. At the third passage, cell exhibited a spindle-shaped, fibroblast-like appearance with a spherical or orbicular-ovate nucleus, as well as rapid proliferation in a whorl-like formation (Fig. 3A). These cells displayed logarithmic proliferation at 4-6 days and the doubling time was 24.37 h (Fig. 3B). Cell surface markers CD29 and CD44 were highly expressed and CD34 and CD45 were minimally expressed in DPSCs (Fig. 3C). To determine the effect of DPSCs on migration and osteoblastic differentiation of

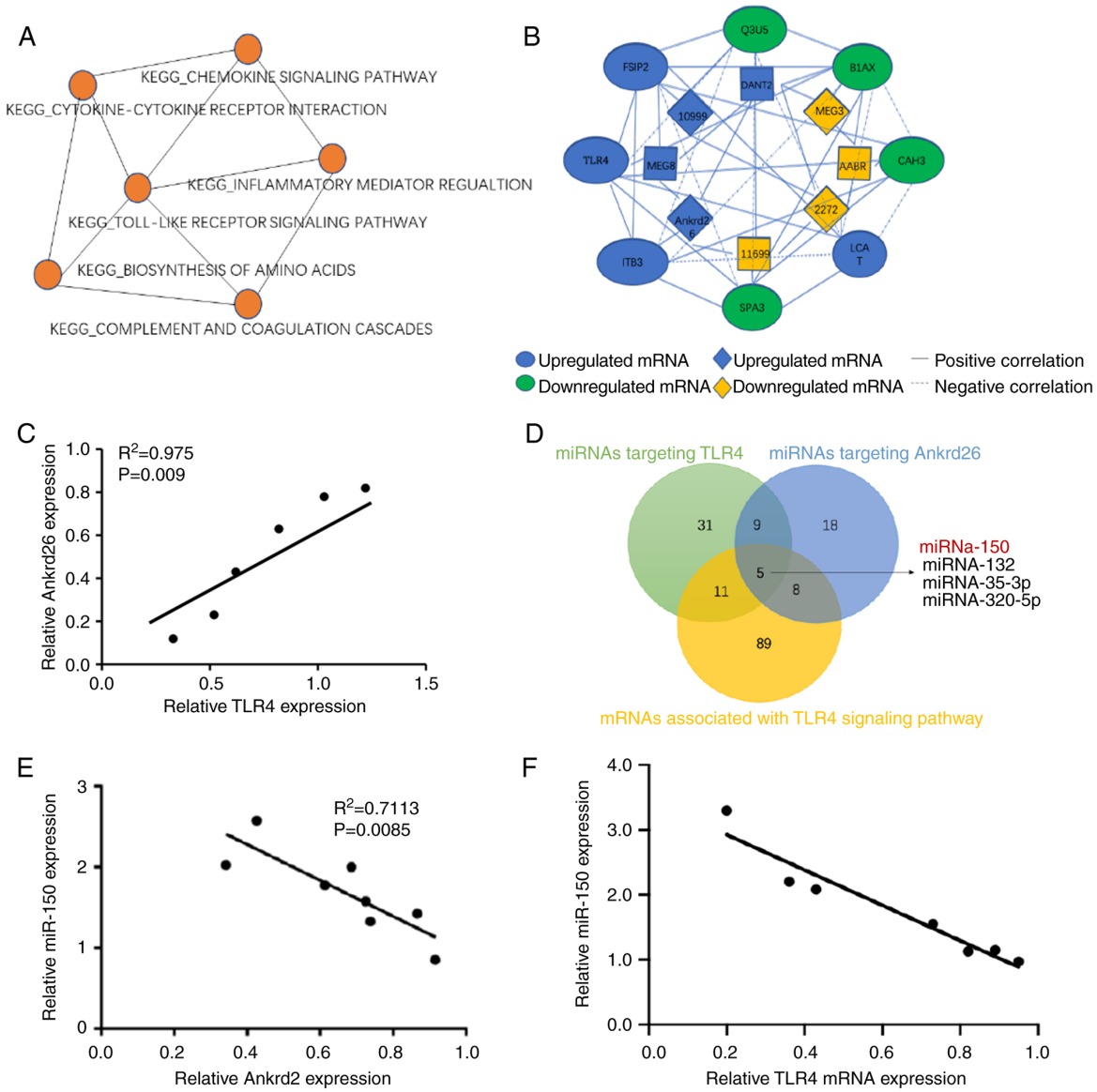

Figure 2. Gene co-expression network and predicted binding sites. (A) Signaling pathway enrichment map. Nodes denote specific gene sets with associated biological function; lines connecting nodes represent overlap based on the of number of genes shared by two gene sets. (B) Gene co-expression network. (C) Relative analysis of lncRNA-Ankrd26 and TLR4. (D) Venn diagram shows common miRNAs that target TLR4 and Ankrd26 simultaneously. Relative expression of (E) lncRNA-Ankrd26 and miRNA-150 and (F) TLR4 and miRNA-150. The results are presented as the mean ± standard deviation. lnc, long non-coding; Ankrd, ankyrin repeat domain; TLR, Toll-like receptor; miRNA, microRNA.

MSCs, MSCs were cultured in conditioned medium from DPSCs. Morphological alteration of MSCs was observed after 4 days as well as significantly increased migration and osteoblastic differentiation with the control (Fig. 3D and E). Due to the association between lncRNA-Ankrd26, TLR4 and miR-150, levels of lncRNA-Ankrd26, TLR4 and miR-150 were measured in MSCs cultured alone or in the conditioned medium from DPSCs. The results showed significantly higher levels of lncRNA-Ankrd26 and TLR4 and significantly lower levels of miR-150 in MSCs with conditioned culture than in MSCs cultured alone (Fig. 3F and G). When exosomal inhibitor (GW4869) was added to the conditioned media, migration and differentiation significantly decreased in MSCs compared with MSCs in conditioned media without GW4869; there was a significant decrease in lncRNA-Ankrd26 and TLR4 and significant increase in miR-150 levels in conditioned culture MSCs with GW4869 compared with those without GW4869 (Fig. 3H-J). These results suggested that DPSC-derived exosomes could promote the migration and osteoblastic differentiation of MSCs.

DPSC-derived exosomal lncRNA-Ankrd26 induces migration and osteoblastic differentiation of MSCs. The present study identified exosomes in medium from DPSCs by TEM (Fig. 4A), which demonstrated positive expression of CD63 and CD81 and negative expression of GM130 and calnexin (Fig. 4B). lncRNA-Ankrd26 expression was significantly increased in DPSC-derived exosomes with lncRNA-Ankrd26 transfection compared with cells without transfection but was markedly inhibited in exosomes when DPSCs were transfected with siRNA targeting lncRNA-Ankrd26 (Fig. 4C and D). Moreover, migration and differentiation significantly decreased in

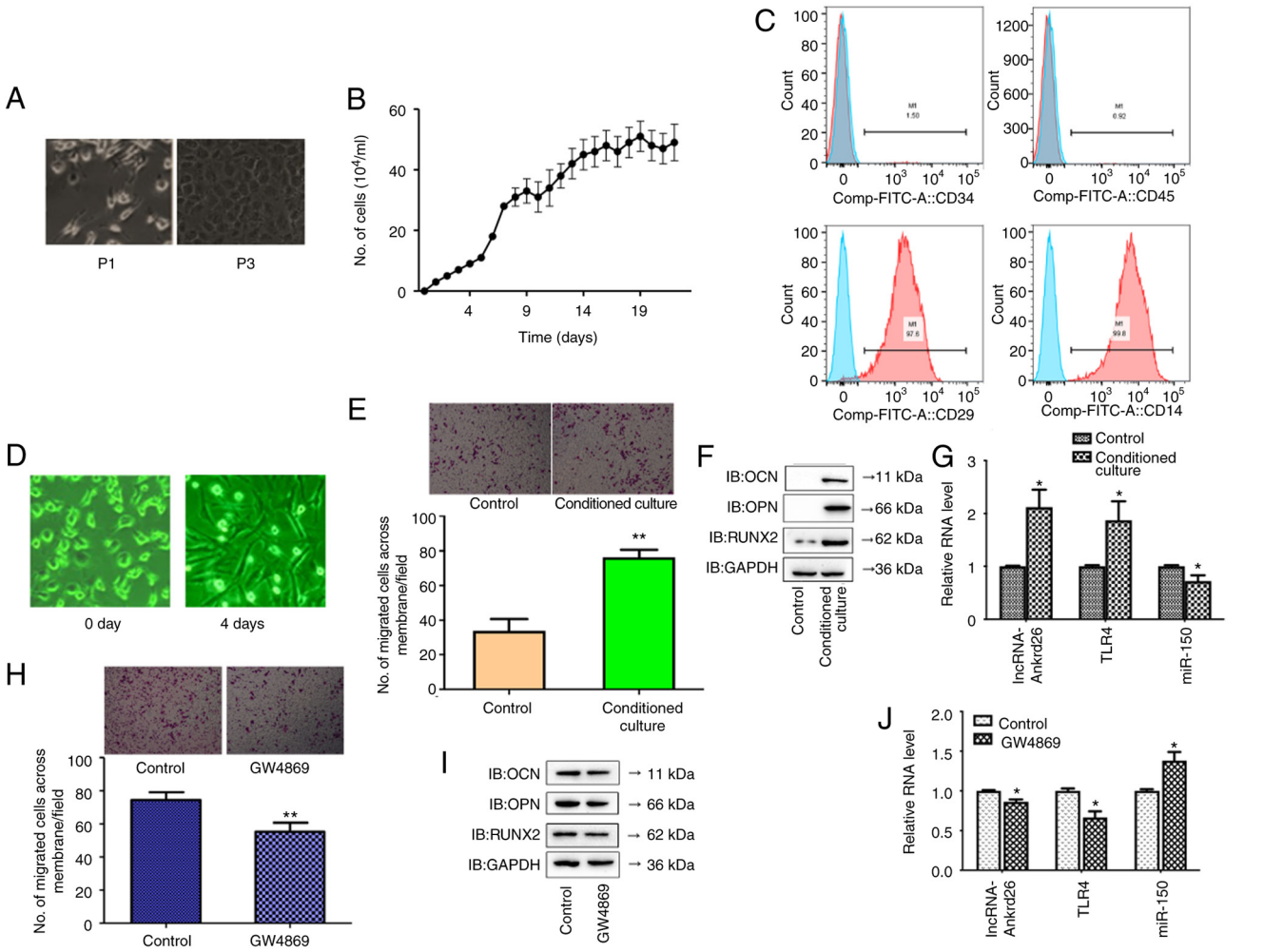

Figure 3. Morphology, propagation, and characterization of DPSCs. (A) Morphology of DPSCs from subcutaneous fat tissue culture *in vitro*. Magnification, x100. (B) Growth curves of DPSCs. (C) Expression of surface antigens (CD29, CD34, CD44, CD45) in DPSCs was detected by flow cytometry. The same negative control (IgG) is included in all plots. (D) Morphological alteration of MSCs after 4 days (x200). (E) Cell migration in MSCs with/without conditioned culture (x100 magnification); **P<0.01 compared with cells without conditioned culture. (F) Protein levels of osteoblastic differentiation-related markers, including OCN, OPN and RUNX2, in MSCs with conditioned culture, compared with control. (G) mRNA levels of lncRNA-Ankrd26, TLR4 and miR-150 in MSCs with conditioned culture. *P<0.05 compared with control. (H) Cell migration in MSCs with/without GW4869 treatment (x100 magnification); **P<0.01 compared with cells without treatment. (I) Protein levels of osteoblastic differentiation-related markers, including OCN, OPN and RUNX2, in MSCs treated with GW4869. (J) mRNA levels of lncRNA-Ankrd26, TLR4 and miR-150 in MSCs treated with GW4869. *P<0.05 compared with control. The results are presented as the mean ± standard deviation. DPSC, dental pulp stem cell; MSC, mesenchymal stem cell; lnc, long non-coding; Ankrd, ankyrin repeat domain; TLR, Toll-like receptor; miR, microRNA; P, passage; IB, immunoblot.

MSCs cultured with conditioned medium from DPSCs with lncRNA-Ankrd26 siRNA transfection compared with MSCs cultured with conditioned medium from DPSCs with control siRNA transfection (Fig. 4E and F). Together, these results suggested that DPSC-mediated promotion of migration and osteoblastic differentiation of MSCs may result from exosomal lncRNA-Ankrd26.

lncRNA-Ankrd26 directly regulates miR-150. A putative binding site of lncRNA-Ankrd26 to miR-150 was mutated and co-transfected with miR-150 mimic into 293T cells (Fig. 5A). Luciferase activity assay demonstrated that, for 293T cells with WT lncRNA-Ankrd26 binding site construct, luciferase reporter activity significantly decreased when cells were transfected with miR-150 mimic compared with cells with miR-NC; Mut binding site construct-transfected cells did not show the significant alteration in the activity regardless of transfection with miR-150 mimic or miR-NC (Fig. 5B). To confirm the role of lncRNA-Ankrd26 in regulating miR-150 expression, anti-AGO2 ribonucleoprotein immunoprecipitation assay was performed using 293T cells transfected with miR-NC or miR-150 mimic and lncRNA-Ankrd26 levels were evaluated by RT-qPCR. The level of lncRNA-Ankrd26 in cells transfected with miR-150 mimic was significantly increased (Fig. 5C). The results suggested that there was a direct interaction between lncRNA-Ankrd26 and miR-150.

Role of exosomal lncRNA-Ankrd26 is dependent on miR-150/TLR4 signaling. The present study confirmed direct binding of miR-150 on the 3'-UTR of TLR4 by dual-luciferase reporter assay. Firstly, by screening targets of miR-150 using Targetscan, TLR4 was identified as a potential target of miR-150 (Fig. 6A). Next, predicted WT or Mut full-length 3'-UTR of TLR4 gene was cloned into a dual-luciferase

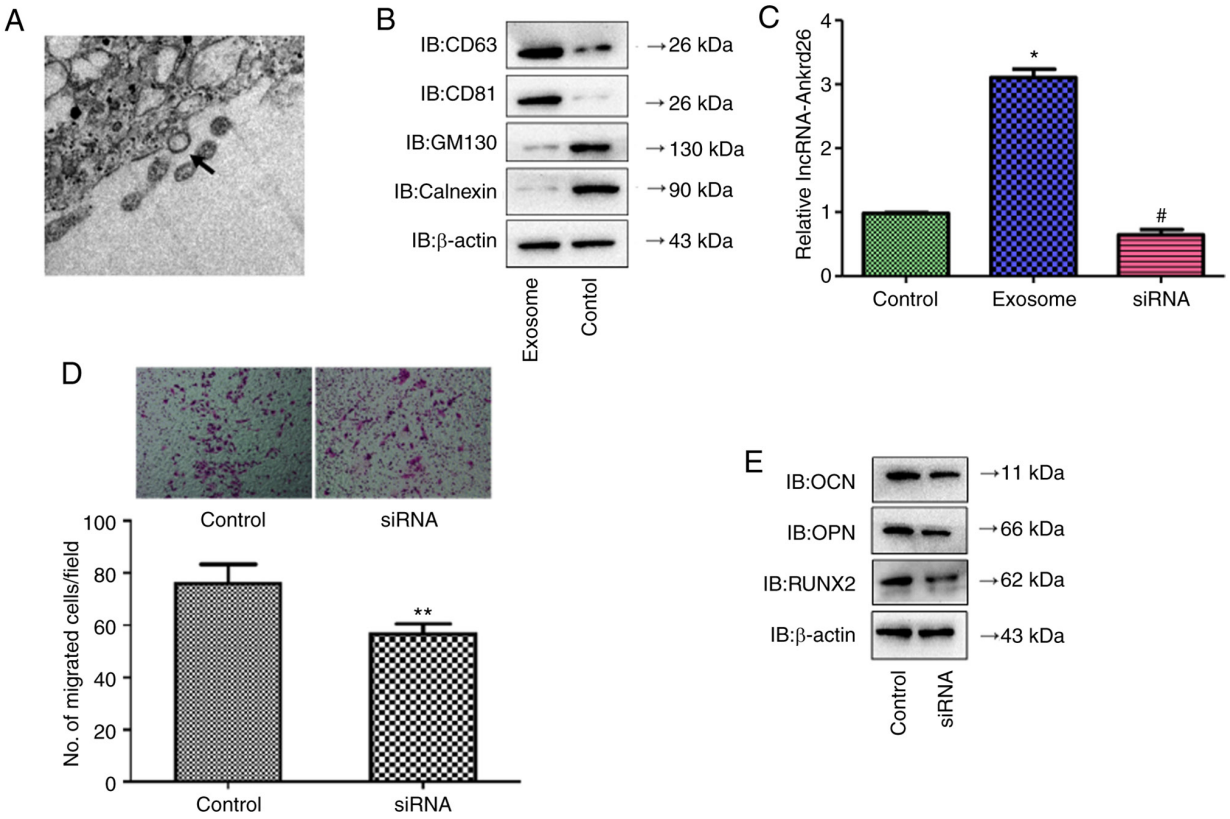

Figure 4. Identification of DPSC-derived exosomes. (A) Exosomes extracted from DPSCs were identified by transmission electron microscopy. Magnification, x150,000. Arrow indicates the representative exosome. (B) Protein levels of CD63, CD81, GM130 and calnexin in DPSC-derived exosomes compared with DPSCs lysate (control) were determined by western blot analysis. (C) lncRNA-Ankrd26 expression was significantly higher in DPSC-derived exosomes with lncRNA-Ankrd26 transfection compared with untransfected cells (control) but was markedly inhibited in exosomes when DPSCs were transfected with siRNA targeting lncRNA-Ankrd26. *P<0.05 compared with control; $^{\#}$P<0.05 compared with exosome. (D) Migration and differentiation significantly decreased in MSCs cultured with conditioned medium from DPSCs with lncRNA-Ankrd26 siRNA transfection compared with MSCs cultured with conditioned medium from DPSCs with control siRNA transfection. **P<0.01 compared with control. (E) Protein levels of osteoblastic differentiation-related markers, including OCN, OPN and RUNX2, in MSCs were determined by western blotting. DPSC, dental pulp stem cell; MSC, mesenchymal stem cell; lnc, long non-coding; Ankrd, ankyrin repeat domain; si, small interfering; IB, immunoblot.

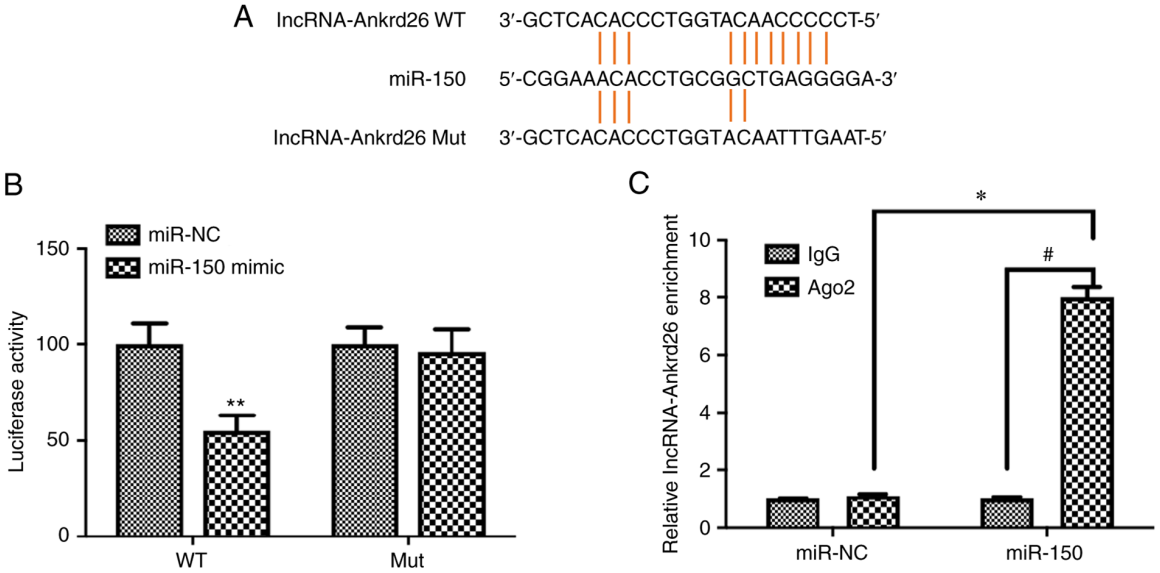

Figure 5. Ankrd26 regulates miR-150. (A) Schematic representation of the predicted binding sites for miR-150 and site mutagenesis design for the reporter assay. (B) Luciferase reporter plasmid containing WT or Mut lncRNA-Ankrd26 was co-transfected into 293T cells with miR-150 mimic or miR-NC treatment. Luciferase activity was determined 48 h after transfection using dual-luciferase assay and to *Renilla* activity. **P<0.01 compared with WT lncRNA-Ankrd26 transfection in 293T cells with miR-NC treatment. (C) Anti-AGO2 ribonucleoprotein immunoprecipitation was performed in 293T cells transfected with miR-150 mimics or miR-NC, followed by reverse transcription-quantitative PCR to detect lncRNA-Ankrd26. *P<0.05 compared with miR-NC; $^{\#}$P<0.05 compared with IgG. The results are presented as the mean ± standard deviation. Ankrd, ankyrin repeat domain; miR, microRNA; WT, wild-type; Mut, mutant; lnc, long non-coding; NC, negative control; AGO2, Argonaute-2.

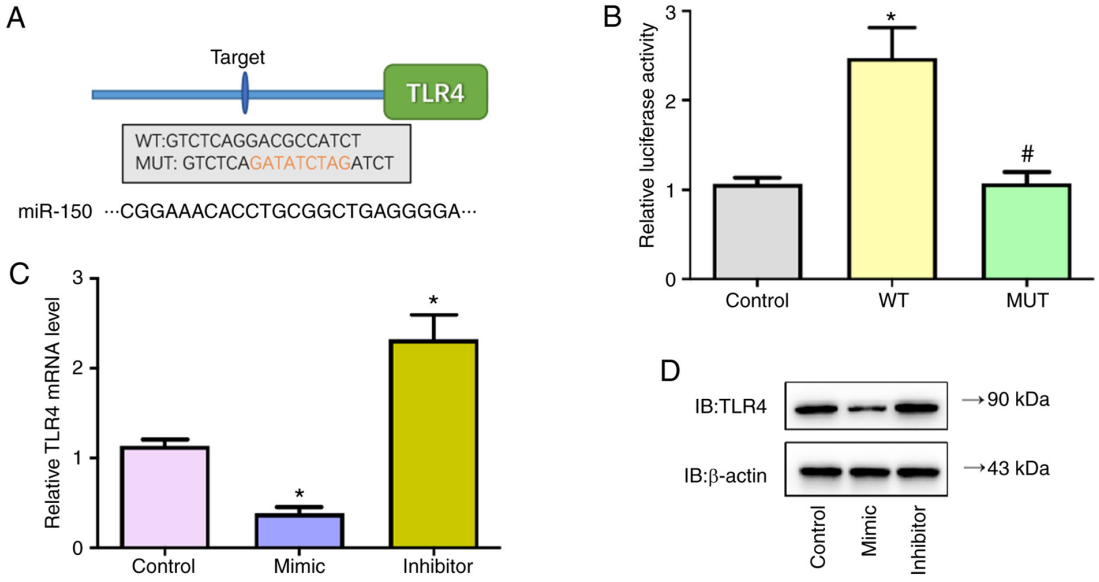

Figure 6. miR-150 regulates TLR4. (A) Schematic representation of the predicted miR-150 binding site in the TLR4 promoter. (B) WT or Mut full-length 3'-UTR of TLR4 gene was inserted into a dual-luciferase reporter plasmid and then co-transfected with miR-150 mimic into 293T cells. *P<0.05 vs. control; #P<0.05 vs. WT. (C) Transcriptional and (D) protein levels of TLR4 in MSC cells with miR-150 mimic, inhibitors or control transfection were detected. The results are presented as the mean ± standard deviation. *P<0.05 vs. control. miR, microRNA; TLR, Toll-like receptor; WT, wild-type; Mut, mutant.

reporter plasmid and then co-transfected with miR-150 mimic into 293T cells. Luciferase activity decreased following miR-150 mimic co-transfection in cells with WT constructs, whereas the activity was not altered in cells co-transfected with Mut constructs (Fig. 6B). In addition, the transcriptional and protein levels of TLR4 in MSC cells transfected with miR-150 mimic, inhibitors or control were detected; miR-150 mimic significantly decreased mRNA and protein levels of TLR4 while miR-150 inhibitors significantly increased levels of TLR4 (Fig. 6C and D). These findings verified that miR-150 negatively regulated TLR4 expression by directly targeting TLR4 in MSC cells.

To investigate whether the role of DPSC-derived exosomal lncRNA-Ankrd26 in inducing migration and osteoblastic differentiation of MSCs required miR-150/TLR4 signaling, TLR4 shRNA was transfected into MSCs. Following transfection, TLR4 mRNA and protein levels were significantly decreased (Fig. 7A and B). TLR4 knockdown notably decreased osteoblastic differentiation markers, including osteocalcin (OCN), osteopontin (OPN) and RUNX2, as well as cell migration (Fig. 7C and D). TLR4-knockdown MSCs cells were cultured in conditioned medium containing DPSC-derived exosomal lncRNA-Ankrd26. When cultured in conditioned medium containing DPSC-derived exosomal lncRNA-Ankrd26, migration and OCN, OPN, RUNX2 expression of MSC cells transfected with control shRNA were significantly increased, but TLR4-knockdown MSC cells displayed no significant change (Fig. 7E and F).

Discussion

DPSCs have been used as key seed cells for pulp regeneration and restoration and exosomes derived from DPSCs have become a research hotspot in pulp regeneration and restoration (19,20). A number of studies have shown that stem cell-derived exosomes are associated with pulp regeneration and inflammation (21-23), suggesting that stem cell-derived exosomes have potential application value in pulp repair and regeneration. Notably, DPSCs hold some advantages, including the fact they are easy to obtain, and their strong proliferation ability and neurotropism (24,25). To the best of our knowledge, however, there are few studies on DPSC-derived exosomes in pulp injury and repair processing. The study demonstrated that DPSC-derived exosomes promoted migration and osteoblastic differentiation of MSCs, which is an important step in the process of dental pulp regeneration and repair. Mechanistically, lncRNA-Ankrd26 served as a competitive endogenous miR-150, regulated differentiation of MSCs via TLR4 signaling and participated in dental pulp regeneration and repair.

As DPSCs have the characteristics of multidirectional differentiation and angiogenesis, the use of DPSCs to regenerate the pulp-dentin complex and repair damaged pulp is expected to become a safe and effective treatment of pulp disease (26,27). Success of periodontal cell-based tissue engineering requires appropriate progenitor cells with the capacity to differentiate into the required mature tissue-forming phenotypes and appropriate signals to modulate cellular differentiation and tissue neogenesis (28). Dental MSCs have the capacity of differentiation into cells that present some characteristics associated with osteoblasts, chondrocytes and adipocytes, thus contributing to tooth growth and repair; easy accessibility of MSCs provides a tractable model system to study their function and properties *in vivo* (27,29). Therefore, MSC-based therapies are being investigated in bone engineering. However, the association between DPSCs and MSCs is still unclear. It has recently been recognized that DPSCs express MSC surface markers, such as CD29, CD44, CD59, CD73, CD90 and CD146, but do not express hematopoietic stem cell markers, such as CD14, CD34, CD45 and CD11b,

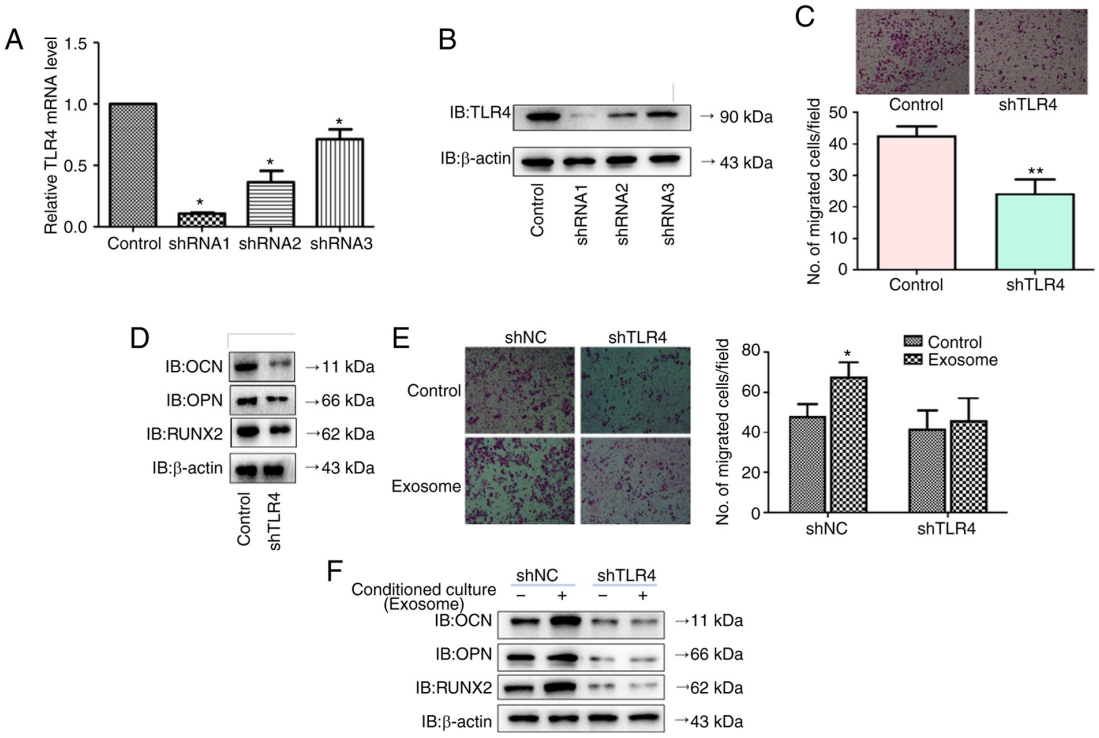

Figure 7. Effects of DPSC-derived exosomal lncRNA-Ankrd26 on MSCs requires the involvement of miR-150/TLR4 signaling. (A) mRNA and (B) protein levels of TLR4 were detected following transfection of TLR4 shRNA into MSCs. *P<0.05 compared with control. (C) Migration (x100 magnification) and (D) osteoblastic differentiation markers, including OCN, OPN and RUNX2, were detected following TLR4 knockdown. **P<0.01 compared with control. (E) Migration (x100 magnification) and (F) osteoblastic differentiation markers, including OCN, OPN and RUNX2, were detected following culture in conditioned medium containing DPSC-derived exosomal lncRNA-Ankrd26. *P<0.05 compared with control. The results are presented as the mean ± standard deviation. DPSC, dental pulp stem cell; MSC, mesenchymal stem cell; lnc, long non-coding; Ankrd, ankyrin repeat domain; sh, short hairpin; IB, immunoblot; miR, microRNA; TLR, Toll-like receptor; OCN, osteocalcin; OPN, osteopontin; NC, negative control.

based on multi-omics analysis (30,31). In the present study, the DPSCs were purified and identified using specific markers. Moreover, the present study used a conditioned culture system and demonstrated that DPSCs promoted migration and osteoblastic differentiation of MSCs, suggesting the importance in understanding the crosstalk between different dental cell populations.

Exosomes serve a key role in regulating cell-cell interaction (32), which confers the possibility of the application of exosomes in the clinical practice of dental disease management. For example, exosomes from DPSCs rescue human dopaminergic neurons from 6-hydroxy-dopamine-induced apoptosis (33) and suppress carrageenan-induced acute inflammation in mice (34), harbor stronger immune-modulating activity (35) and trigger regeneration of dental pulp-like tissue (30). Consistently, DPSC promotion of migration and osteoblastic differentiation of MSCs is mediated by exosomes. To the best of our knowledge, the present study is the first to report the association between DPSC-derived exosomes and MSC differentiation.

To facilitate intercellular communication, exosomes contain RNA and proteins (36). Previous studies have demonstrated that exosomes participate in epithelium-mesenchyme crosstalk in tooth morphogenesis and differentiation by transferring RNA to recipient cells (37-39). Moreover, the present study demonstrated that DPSC-derived exosomal lncRNA-Ankrd26 induced migration and osteoblastic differentiation of MSCs by regulating miR-150/TLR4 signaling, as shown by analysis dysregulated mRNAs, lncRNAs and TLR signaling pathway during the repair and regeneration of damaged dental pulp. The present study verified that lncRNA-Ankrd26 directly regulated miR-150 in MSCs. To the best of our knowledge, the present study is the first to clarify the association between lncRNA Ankrd26 and miR-150 in osteoblast differentiation and tissue restoration. The present study confirmed the hypothesis that DPSC-derived exosomal lncRNA-Ankrd26 promotion of migration and osteoblastic differentiation in MSCs was dependent on of miR-150/TLR4 signaling. To the best of our knowledge, the present study is the first to demonstrate the association between lncRNA-Ankrd26 and dental pulp repair. ANKRD26 gene silencing and variation are associated with regulation of pro-inflammatory factors (40), platelet aggregation (41) and adipogenesis (42). TLR signaling is a key mediator for inflammatory pathways and tissue response to both pathogen- and damage-associated molecular pattern factors (43). TLR4, a key component of TLR family, serves a role in wound healing (44). TLR4 activation in MSCs mediates production of multiple cytokines, chemokines and inflammatory mediators, thus contributing to osteoclastogenesis (45). Enhancement of TLR4 activity increases osteoblast viability (46) and differentiation of adipose-derived stem cells (47). These aforementioned studies suggested that TLR4 modulates inflammation-induced healing response in different clinical settings.

There are certain limitations in the present study. Cell-derived exosomes contain a variety of components including inflammatory and growth factors, genetic material and

lipids (13,14). Although the present study demonstrated the role of DPSC-derived exosomal lncRNA-Ankrd26-miR-150-TLR4 signaling in regulating migration and osteoblastic differentiation of MSCs in pulp regeneration and restoration, other exosomal content may serve a role in crosstalk between DPSCs and MSC. Secondly, the present study used cells from model animals, which may be not accurately represent human disease. Moreover, due to the limitations in clinical feasibility, pulp tissue was used as control; however, control pulp tissue was not active in pulp restoration. Patient-derived xenografts or more appropriate cell models *in vitro* will be used in future. In addition, the present study only investigated the role of miR-150/TLR4 signaling in terms of the effects of DPSC exosomal lncRNA-Ankrd26 on inducing migration and osteoblastic differentiation of MSCs. Further studies are required to characterize the mechanism by which exosomes control the migration and osteoblastic differentiation of MSCs in pulp regeneration and restoration. Nevertheless, the present results support an important potential role for DPSC-derived exosomal lncRNA-Ankrd26 in promoting migration and osteoblastic differentiation of MSCs. Moreover, considering previous advances in miRNA-mediated therapy in tissue regeneration and restoration (48-50), lncRNA-Ankrd26 may be a potential target for patients with dental pulp inflammation.

In summary, the present study investigated the role of lncRNA/Ankrd26/miR-150-TLR4 signaling in differentiation of stem cells, which will provide understanding of the molecular mechanism in dental pulp regeneration and restoration.

Acknowledgements

The authors would like thank Dr Yang Zhang (Fudan University) for help in depositing the original data to a public database.

Funding

The present study was supported by the Fund of Stomatology Hospital Affiliated to Tongji University (grant no. 20183001).

Availability of data and materials

The datasets generated and/or analyzed during the current study are available in the NCBI BIOSAMPLE repository (ncbi.nlm.nih.gov/sra; accession no. PRJNA767485).

Authors' contributions

JG conceived and designed the study. LL and JG analyzed the data, performed experiments and drafted the manuscript. Both authors have read and approved the final manuscript. LL and JG confirm the authenticity of all the raw data.

Ethics approval and consent to participate

All animal studies were approved by the Institutional Animal Care and Use Committees of the Hospital of Stomatology, Tongji University (approval no. 20180606; Jan 1, 2018), in compliance with the Basel Declaration and institutional guidelines for the care and use of animals.

Patient consent for publication

Not applicable.

Competing interests

The authors declare that they have no competing interests.

References

1. Yamada Y, Nakamura-Yamada S, Kusano K and Baba S: Clinical potential and current progress of dental pulp stem cells for various systemic diseases in regenerative medicine: A concise review. Int J Mol Sci 20: 1132, 2019.
2. Chauhan R, Rasaratnam L, Alani A and Djemal S: Adult dental trauma: What should the dental practitioner know? Prim Dent J 5: 70-81, 2016.
3. Mead B, Logan A, Berry M, Leadbeater W and Scheven BA: Concise review: Dental pulp stem cells: A novel cell therapy for retinal and central nervous system repair. Stem Cells 35: 61-67, 2017.
4. Gronthos S, Mankani M, Brahim J, Robey PG and Shi S: Postnatal human dental pulp stem cells (DPSCs) in vitro and in vivo. Proc Natl Acad Sci USA 97: 13625-13630, 2000.
5. Yang R, Liu Y, Yu T, Liu D, Shi S, Zhou Y and Zhou Y: Hydrogen sulfide maintains dental pulp stem cell function via TRPV1-mediated calcium influx. Cell Death Discov 4: 69, 2018.
6. Munévar JC, Gutiérrez N, Jiménez NT and Lafaurie GI: Evaluation of two human dental pulp stem cell cryopreservation methods. Acta Odontol Latinoam 28: 114-121, 2015.
7. Tatsuhiro F, Seiko T, Yusuke T, Reiko TT and Kazuhito S: Dental pulp stem cell-derived, scaffold-free constructs for bone regeneration. Int J Mol Sci 19: 1846, 2018.
8. Wang J, Ma H, Jin X, Hu J, Liu X, Ni L and Ma PX: The effect of scaffold architecture on odontogenic differentiation of human dental pulp stem cells. Biomaterials 32: 7822-7830, 2011.
9. Kichenbrand C, Velot E, Menu P and Moby V: Dental pulp stem cell-derived conditioned medium: An attractive alternative for regenerative therapy. Tissue Eng Part B Rev 25: 78-88, 2019.
10. Morsczeck C and Reichert TE: Dental stem cells in tooth regeneration and repair in the future. Expert Opin Biol Ther 18: 187-196, 2018.
11. Iezzi I, Pagella P, Mattioli-Belmonte M and Mitsiadis TA: The effects of ageing on dental pulp stem cells, the tooth longevity elixir. Eur Cell Mater 37: 175-185, 2019.
12. Schuh CMAP, Benso B and Aguayo S: Potential Novel Strategies for the treatment of dental pulp-derived pain: Pharmacological approaches and beyond. Front Pharmacol 10: 1068, 2019.
13. Chen T, Moscvin M and Bianchi G: Exosomes in the pathogenesis and treatment of multiple myeloma in the context of the bone marrow microenvironment. Front Oncol 10: 608815, 2020.
14. Li Y, Yin Z, Fan J, Zhang S and Yang W: The roles of exosomal miRNAs and lncRNAs in lung diseases. Signal Transduct Target Ther 4: 47, 2019.
15. Asgarpour K, Shojaei Z, Amiri F, Ai J, Mahjoubin-Tehran M, Ghasemi F, ArefNezhad R, Hamblin MR and Mirzaei H: Exosomal microRNAs derived from mesenchymal stem cells: Cell-to-cell messages. Cell Commun Signal 18: 149, 2020.
16. Xu Y, Xiao Q, Tian H, Zhang L and Zhang G: Biological effects of the extracellular matrix on rat bone marrow mesenchymal stem cells. Chin J Curr Adv Gen Surg 10: 26-29, 2007 (In Chinese).
17. Shu S, Yang Y, Allen CL, Maguire O, Minderman H, Sen A, Ciesielski MJ, Collins KA, Bush PJ, Singh P, *et al*: Metabolic reprogramming of stromal fibroblasts by melanoma exosome microRNA favours a pre-metastatic microenvironment. Sci Rep 8: 12905, 2018.
18. Livak KJ and Schmittgen TD: Analysis of relative gene expression data using real-time quantitative PCR and the 2(-Delta Delta C(T)) method. Methods 25: 402-408, 2001.
19. Huang CC, Narayanan R, Alapati S and Ravindran S: Exosomes as biomimetic tools for stem cell differentiation: Applications in dental pulp tissue regeneration. Biomaterials 111: 103-115, 2016.
20. Hu X, Zhong Y, Kong Y, Chen Y, Feng J and Zheng J: Lineage-specific exosomes promote the odontogenic differentiation of human dental pulp stem cells (DPSCs) through TGFβ1/smads signaling pathway via transfer of microRNAs. Stem Cell Res Ther 10: 170, 2019.

21. Yu B, Zhang X and Li X: Exosomes derived from mesenchymal stem cells. Int J Mol Sci 15: 4142-4157, 2014.
22. Hao ZC, Lu J, Wang SZ, Wu H, Zhang YT and Xu SG: Stem cell-derived exosomes: A promising strategy for fracture healing. Cell Prolif 50: e12359, 2017.
23. Mendt M, Rezvani K and Shpall E: Mesenchymal stem cell-derived exosomes for clinical use. Bone Marrow Transplant 54 (Suppl 2): S789-S792, 2019.
24. Sharma A: Role of stem cell derived exosomes in tumor biology. Int J Cancer 142: 1086-1092, 2018.
25. Harrell CR, Jovicic N, Djonov V, Arsenijevic N and Volarevic V: Mesenchymal stem cell-derived exosomes and other extracellular vesicles as new remedies in the therapy of inflammatory diseases. Cells 8: 1605, 2019.
26. Zhai Q, Dong Z, Wang W, Li B and Jin Y: Dental stem cell and dental tissue regeneration. Front Med 13: 152-159, 2019.
27. Hu L, Liu Y and Wang S: Stem cell-based tooth and periodontal regeneration. Oral Dis 24: 696-705, 2018.
28. Han J, Menicanin D, Gronthos S and Bartold PM: Stem cells, tissue engineering and periodontal regeneration. Aust Dent J 59 (Suppl 1): S117-S130, 2014.
29. Sharpe PT: Dental mesenchymal stem cells. Development 143: 2273-2280, 2016.
30. Stanko P, Altanerova U, Jakubechova J, Repiska V and Altaner C: Dental mesenchymal stem/stromal cells and their exosomes. Stem Cells Int 2018: 8973613, 2018.
31. Cui D, Li H, Wan M, Peng Y, Xu X, Zhou X and Zheng L: The origin and identification of mesenchymal stem cells in teeth: From odontogenic to non-odontogenic. Curr Stem Cell Res Ther 13: 39-45, 2018.
32. Mathieu M, Martin-Jaular L, Lavieu G and Théry C: Specificities of secretion and uptake of exosomes and other extracellular vesicles for cell-to-cell communication. Nat Cell Biol 21: 9-17, 2019.
33. Jarmalavičiūtė A, Tunaitis V, Pivoraitė U, Venalis A and Pivoriūnas A: Exosomes from dental pulp stem cells rescue human dopaminergic neurons from 6-hydroxy-dopamine-induced apoptosis. Cytotherapy 17: 932-939, 2015.
34. Pivoraitė U, Jarmalavičiūtė A, Tunaitis V, Ramanauskaitė G, Vaitkuvienė A, Kašėta V, Biziulevičienė G, Venalis A and Pivoriūnas A: Exosomes from human dental pulp stem cells suppress carrageenan-induced acute inflammation in mice. Inflammation 38: 1933-1941, 2015.
35. Ji L, Bao L, Gu Z, Zhou Q, Liang Y, Zheng Y, Xu Y, Zhang X and Feng X: Comparison of immunomodulatory properties of exosomes derived from bone marrow mesenchymal stem cells and dental pulp stem cells. Immunol Res 67: 432-442, 2019.
36. van der Grein SG and Nolte-'t Hoen EN: 'Small Talk' in the Innate immune system via RNA-containing extracellular vesicles. Front Immunol 5: 542, 2014.
37. Colombo M, Raposo G and Théry C: Biogenesis, secretion, and intercellular interactions of exosomes and other extracellular vesicles. Annu Rev Cell Dev Biol 30: 255-289, 2014.
38. Jiang N, Xiang L, He L, Yang G, Zheng J, Wang C, Zhang Y, Wang S, Zhou Y, Sheu TJ, *et al*: Exosomes mediate epithelium-mesenchyme crosstalk in organ development. ACS Nano 11: 7736-7746, 2017.
39. Nakao Y, Fukuda T, Zhang Q, Sanui T, Shinjo T, Kou X, Chen C, Liu D, Watanabe Y, Hayashi C, *et al*: Exosomes from TNF-α-treated human gingiva-derived MSCs enhance M2 macrophage polarization and inhibit periodontal bone loss. Acta Biomater 122: 306-324, 2021.
40. Desiderio A, Longo M, Parrillo L, Campitelli M, Cacace G, de Simone S, Spinelli R, Zatterale F, Cabaro S, Dolce P, *et al*: Epigenetic silencing of the ANKRD26 gene correlates to the pro-inflammatory profile and increased cardio-metabolic risk factors in human obesity. Clin Epigenetics 11: 181, 2019.
41. Chen MH, Yanek LR, Backman JD, Eicher JD, Huffman JE, Ben-Shlomo Y, Beswick AD, Yerges-Armstrong LM, Shuldiner AR, O'Connell JR, *et al*: Exome-chip meta-analysis identifies association between variation in ANKRD26 and platelet aggregation. Platelets 30: 164-173, 2019.
42. Fei Z, Bera TK, Liu X, Xiang L and Pastan I: Ankrd26 gene disruption enhances adipogenesis of mouse embryonic fibroblasts. J Biol Chem 286: 27761-27768, 2011.
43. McKeown-Longo PJ and Higgins PJ: Integration of canonical and noncanonical pathways in TLR4 signaling: Complex regulation of the wound repair program. Adv Wound Care (New Rochelle) 6: 320-329, 2017.
44. Bhattacharyya S and Varga J: Endogenous ligands of TLR4 promote unresolving tissue fibrosis: Implications for systemic sclerosis and its targeted therapy. Immunol Lett 195: 9-17, 2018.
45. Alonso-Pérez A, Franco-Trepat E, Guillán-Fresco M, Jorge-Mora A, López V, Pino J, Gualillo O and Gómez R: Role of toll-like receptor 4 on osteoblast metabolism and function. Front Physiol 9: 504, 2018.
46. Zheng L, Shen X, Ye J, Xie Y and Yan S: Metformin alleviates hyperglycemia-induced apoptosis and differentiation suppression in osteoblasts through inhibiting the TLR4 signaling pathway. Life Sci 216: 29-38, 2019.
47. Yu L, Qu H, Yu Y, Li W, Zhao Y and Qiu G: LncRNA-PCAT1 targeting miR-145-5p promotes TLR4-associated osteogenic differentiation of adipose-derived stem cells. J Cell Mol Med 22: 6134-6147, 2018.
48. Olsen I, Singhrao SK and Osmundsen H: Periodontitis, pathogenesis and progression: miRNA-mediated cellular responses to porphyromonas gingivalis. J Oral Microbiol 9: 1333396, 2017.
49. Irhimeh MR, Hamed M, Barthelmes D, Gladbach Y, Helms V, Shen W and Gillies MC: Identification of novel diabetes impaired miRNA-transcription factor co-regulatory networks in bone marrow-derived Lin-/VEGF-R2+ endothelial progenitor cells. PLoS One 13: e0200194, 2018.
50. Kadota T, Fujita Y, Araya J, Watanabe N, Fujimoto S, Kawamoto H, Minagawa S, Hara H, Ohtsuka T, Yamamoto Y, *et al*: Human bronchial epithelial cell-derived extracellular vesicle therapy for pulmonary fibrosis via inhibition of TGF-β-WNT crosstalk. J Extracell Vesicles 10: e12124, 2021.